Line-narrowed electro-optic periodically-poled-lithium-niobate Q-switched laser with intra-cavity optical parametric oscillation using a grazing-incidence grating

An-Chung Chiang (蔣安忠)[1] and Yen-Yin Lin (林彥穎)[2]

[1]*Nuclear Science and Technology Development Center, National Tsinghua University, Hsinchu 30013, China,*

[2]*Institute of Photonics Technology, National Tsinghua University, Hsinchu 30013, China*

[*]*Corresponding author: acchiang@mx.nthu.edu.tw*

Received December 17, 2013; accepted January 22, 2014; posted online March 12, 2014

We report a line-narrowed electro-optic periodically-poled-lithium-niobate (PPLN) Q-switched laser with intra-cavity optical parametric oscillation using a grazing-incidence grating, producing 8-ns, 5-μJ pulses at 10-kHz repetition rate when pumped with a 10-W diode laser at 808 nm. The output wavelength is centered at 1554.3 nm with a 0.03-nm spectral width. Wavelength tuning is achieved by rotating a mirror and changing the crystal temperature.

OCIS codes: 140.3480, 140.3540, 190.4975.

doi: 10.3788/COL201412.041401.

High-power wavelength-tunable laser sources in the infrared region are desired for plenty of applications, especially in the fields of spectroscopy and molecular detection. Among those applications, narrow linewidths are often important and necessary. Such laser sources are usually complex and expensive. In the past decade, development shows that periodically-poled-lithium-niobate (PPLN) based lasers are very promising for such applications. Lithium niobate has good transparency from the visible to the mid-infrared region, and is extensively used in a variety of nonlinear-frequency-mixing processes with the quasi-phase-matching (QPM) technique[1,2]. Recently, PPLN applications have been extended to the fields of high-speed communications and advanced laser technologies based on the highly engineerable nonlinear optical characteristics[3,4]. Despite nonlinear frequency mixing, PPLN was also demonstrated to be a good device for laser Q-switching based on its electro-optic (EO) properties and Bragg diffraction[5−7].

In our previous work, we successfully demonstrated a compact and wavelength-tunable PPLN EO Q-switched laser with intra-cavity optical parametric generation (OPG)[8,9]. However, the spectral width of the output wavelength was 3-5 nm, which was a typical number that comes from Q-switched laser pumped PPLN OPG[10]. Intra-cavity dispersive elements, such as an etalon[11] or a grating can help to control the spectral width, but will greatly introduce optical loss to the laser cavity and increase the threshold power. The wavelength tuning is also inconvenient if intra-cavity elements are inserted.

Considering easy-alignment, tuning-capability, and low intra-cavity loss, it is straight-forward that we use the configuration with a grazing incident grating[12]. Therefore, we designed and demonstrated a line-narrowed EO PPLN Q-switched laser with intra-cavity optical parametric oscillation (OPO) using a grazing incidence grating. Excluding the pumping laser, the system is within a 5×5 (inch) area. We used MgO-doped PPLN crystals in the experiment for avoiding photo-refraction which usually occurs in congruent lithium niobate and cause instability to the laser performance[13].

Figure 1 shows the experimental setup. The system is a L-folded structure, consisting of a pump laser source, a set of coupling lenses, a Nd:YVO_4 crystal, a PPLN Bragg modulator, a mode-shaping lens, a 45° flat mirror, an OPO PPLN crystal, a concave mirror as a back reflector, and a grazing-incidence-grating-mirror combination.

The pump laser source is a 20-W diode laser at 808 nm, pigtailed by a multi-mode silica fiber with an 800-μm core diameter and a 0.18 numerical aperture (NA). The 808-nm laser was coupled from the fiber output to the center of the Nd:YVO_4 crystal through a set of coupling lenses with a one-to-one imaging ratio.

The Nd:YVO_4 crystal is a 9-mm-long, a-cut 0.25 at.-% Nd-doped YVO_4 crystal with its end surfaces coated with anti-reflection layers at both 1064 and 808 nm. The side surfaces of the Nd:YVO_4 crystal was wrapped in an indium foil and mounted in a water-cooled copper housing to dissipate excess heat. Heat dissipation ensured the stability of the 1064-nm fundamental laser power.

The S1 surface of the coupling lens is high-reflection coated at 1064 nm ($R > 99.8\%$) and high-transmission coated at 808 nm ($T > 90\%$). The back reflector is a CaF_2 concave mirror which allows mid-infrared radiation passing through it. The concave side (S2) of the back reflector has a radius of curvature of 100 mm and is high-reflection coated at 1064 nm ($R > 99.7\%$) and high-reflection coated during 1400-1600 nm ($R > 99\%$). The broad-band high-reflection coating makes the wavelength tuning capability possible.

The 45° flat mirror is high-reflection coated at 1064 nm ($R > 99.7\%$) and anti-reflection coated during 1400-1600 nm ($T > 95\%$). Therefore, the 1064-nm laser wavelength is designed to be oscillated between S1 and S2; and the optical parametric signal wave is designed

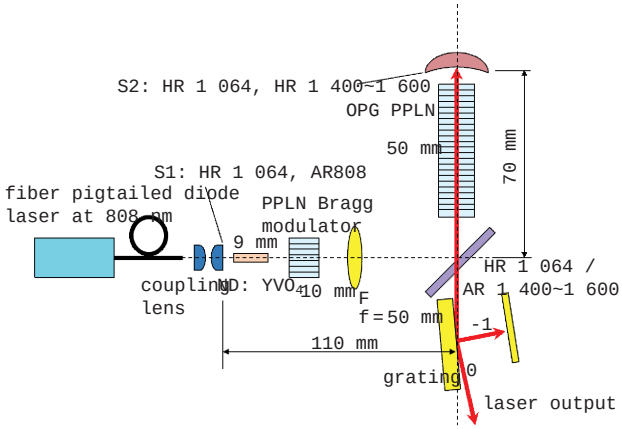

Fig. 1. Schematic setup of the line-narrowed PPLN Q-switched laser with intra-cavity OPO using a grazing-incidence grating. The 1064-nm laser wavelength is oscillated between S1 and S2 surfaces; the optical parametric signal is oscillated between S2 surface and the grating-mirror combination. The laser output is along the direction of the 0th order diffraction.

to be passing through the 45° flat mirror, and is oscillated between S2 surface and the grating-mirror combination. The 45° flat mirror has a cut-off wavelength at 3-μm. Wavelength longer than 3 μm cannot pass through this mirror.

The double convex lens F (f=50 mm) is anti-reflection coated at 1064 nm on its both surfaces. This lens not only ensures a good focusing condition for the optical parametric process and also keeps a divergence-less laser mode inside the PPLN Bragg modulator. According to our design, the 1/e-square laser radius inside the OPO PPLN crystal is 110 μm. For the PPLN Bragg modulator, the laser radius inside it is 170 μm and the diverging angle is 4 mrad. Clipping loss is also avoided under such conditions. For the ease of alignment, we proceeded laser mode simulation and found a suitable design of the cavity mode which is always stable with and without the OPO PPLN crystal; therefore, we can firstly align the PPLN Q-switched laser and then insert the OPO PPLN crystal. If the OPG PPLN crystal is removed, the laser system can be operated as a 1064-nm Q-switched Nd:YVO_4 laser without doing any modification.

In the experiment, we used MgO:PPLN crystal as the intra-cavity frequency convertor, which has the dimension of 50 × 5.2 × 1 (mm). This MgO:PPLN crystal is multiple-grating and comprises seven PPLN gratings arranged parallel to the laser beam. The seven gratings have periods of 28.5, 29, 29.5, 30, 30.5, 31, and 31.5 μm, each with a width of 0.7 mm, with 0.05-mm separation between adjacent gratings. When the crystal is pumped by 1064-nm laser radiations, the multiple-grating structure can produce OPG signal wavelengths from 1.45 to 2.128 μm and idler wavelength from 3.99 to 2.128 μm, respectively, with the crystal temperature tuned from 25 to 165 °C. Although the system is wavelength tunable, we focus on the spectral narrowing phenomenon and only the 30-μm PPLN grating was used. The crystal temperature is near 25 °C.

We also used a MgO:PPLN crystal as the PPLN Bragg modulator. The transverse width along crystalline y direction is 10 mm and the thickness along the z direction is 0.78 mm. The grating period is 20.3 μm. The $\pm z$ surfaces of the first PPLN Bragg modulator were coated with 50-nm-thick NiCr electrodes, on which a voltage was applied to form a Bragg grating during the high-loss state of laser Q-switching. According to our measurement, the normalized half-wave voltage of the PPLN Bragg modulator is 0.3 $V \times d$ (μm) / L (cm). This value is slightly larger than a conventional EO PPLN Pockels cell due to the deviation from the 50 % ideal PPLN duty cycle. Driving the PPLN Bragg modulator as the laser Q-switch, we applied a 10-kHz driving voltage pulses to the PPLN Bragg modulator. We biased the PPLN to −140 V and applied the +140 V, 300-ns voltage pulse to it. Alternately speaking, we applied a long duty-cycle and negative driving pulse to the Bragg modulator. The rise time of the voltage pulse is less than 10 ns.

The grating-mirror combination consists of a gold coated grating and a gold coated flat reflector. The gold coated grating is a standard ruled grating blazed at 29°52′ with a dimension of 25 × 25 × 9.5 (mm). The groove density was 830 grooves/mm. With the grazing incidence configuration, the optical parametric signal wave propagated nearly parallel to the grating surface and was diffracted to the -1st order direction which was nearly normal to the grating surface, and was reflected by the gold coated flat reflector to its coming direction. The grating was fixed at an 88° of incidence angle for a fixed output spectral width. The flat reflector was mounted on a motorized rotation stage. The overall reflectance (including the forward and the backward directions) of the -1st order diffraction beam was measured to be 20 %. The signal energy was coupled out from the zeroth-order diffraction of the grating.

Figure 2 shows the pumping power versus output energy with and without the grating-mirror combination, respectively. Under room temperature operation, the system worked with low energy fluctuation. By taking averaging data for 1 minute, the energy fluctuation ((max-min)/average) is less than 5 %. Without the grating-mirror combination, the threshold power of the PPLN intra-cavity OPG was 2.6 W. When the pump power was 10 W, the system produced 10.1-μJ OPG pulses at 10 kHz. The measured pulse width was 8 ns.

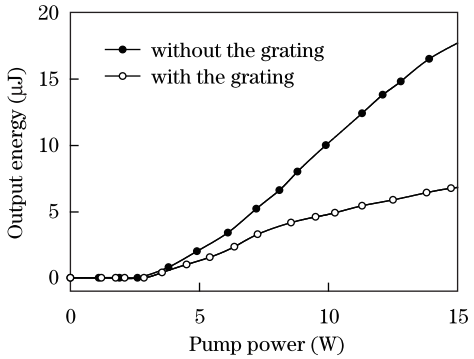

Fig. 2. Output energy versus pump power. Without the grating-mirror combination, the signal energy is 10.1 μJ under 10-W pump power. When the pump power exceeds 10 W, multi-pulse generation is observed. The measured energy is the sum of all pulses in a period. The produced wavelength is 1554.3 nm. With the grating, the output energy dropped by a factor of 2.

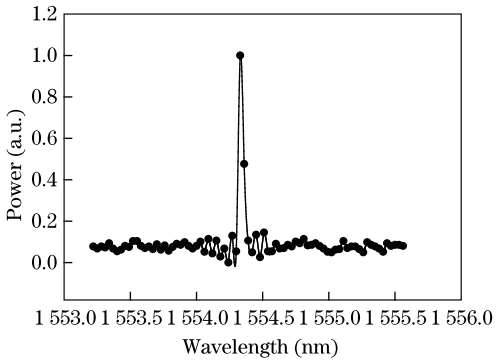

Fig. 3. Spectral width of the signal pulse with the grazing-incidence grating. With 10-W pump power, the signal pulse energy is 5 μJ at 10-kHz repetition rate. The spectral width is measured by a grating monochromator and shows a 0.03-nm (FWHM) width. The central wavelength is 1554.3 nm and the PPLN temperature is 25 °C.

When the pump power was continuously increased (> 10 W), the repetitive pulsing regime was observed[14]. Multiple pulses were generated in one period. The measured output energy was the sum of all the multiple pulses when the pump power exceeded 10 W. This is due to the extremely high gain inside the laser cavity and can be commonly found in various intra-cavity applications. For reducing the number of pulses, we can simply introduce losses to the laser cavity, such as slightly misaligning the cavity or using output coupling mirrors, instead of the high-reflection back reflectors, to release the 1064-nm intra-cavity power. However, for evaluating the contribution of the grating-mirror combination, we did not precede the cavity adjustment.

With the grating-mirror combination, the threshold of the system remained unchanged but the output pulse energy dropped by a factor of 2, while the pulse width remained similar with the result without the grating-mirror combination. The onset of intra-cavity parametric processes strongly relies on the intra-cavity power of the 1064-nm fundamental waves. Once the fundamental laser reached its threshold, it instantaneously generated high intra-cavity power and provided sufficient parametric gain. The grating-mirror combination provided spectrally controlled seeding power to the amplification process and concentrated the parametric gain into the limited spectral range. As long as the 1064-nm laser reached its threshold, both the seeded and unseeded parametric process would start. This explains the unchanged threshold. The grating-mirror combination not only provided unstable mode for the parametric signal, but also generated angular dispersion. Since signal mode was inconsistent with the 1064-mode and much larger than it, only a small portion of the seeding power was amplified. For the unseeded process, all the vacuum noises within the gain bandwidth were amplified. With the limitation of the bandwidth, the grating mirror combination resulted in less efficiency but higher energy per unit spectral width.

The spectral width was found to be significantly narrowed. In determining the spectral width, we used a grating monochromator with a maximum resolution of 0.03 nm. During the measuring process, we scanned the spectral range near the central wavelength (1554.3 nm) and averaged each data points for 1 second. Without the grating-mirror combination, the full-width at half-maximum (FWHM) spectral width of the output signal was 4 nm and would slightly increase with the pump power. With the grating-mirror combination, the measured FWHM spectral width was about 0.03 nm. Figure 3 shows the result of the spectral measurement with the grazing incidence grating. However, we would not know the exact spectral width since this number was beyond the maximum resolution of the grating monochromator. It is possible to measure the exact the spectral width by using a scanning Fabry-Perot interferometer in the future.

Without the grazing-incidence grating, the signal wavelength was tuned well with the predicted calculation by tuning the temperature and the grating period of the PPLN crystal based on the phase matching condition and the Sellmeier coefficients of MgO doped lithium niobate[15]. We efficiently produced tunable laser radiations from 1450 to 1600 nm. For the wavelengths longer than 1600 nm, the efficiency significantly decreased due to the lack of optical feedback provided by the S2 high reflector. With the grating-mirror combination, wavelength tuning was achieved by adjusting the angle of the rear reflector of the grating-mirror combination. For the 30-μm grating period at 25 °C, the output wavelength centered at 1554.3 nm, the tuning rate was 1.4nm/mrad. The tuning range was about 4 nm, which corresponds to the signal spectral width without the grating. Changing the crystal temperature gave more tuning range but the angle of the rear reflector needed to be changed accordingly. Although the wavelength tuning method is not as simple as that of a normal QPM OPG or OPO system, it is still very comfortable for most applications which require high-power, narrow-line, and tunable laser sources.

In conclusion, we demonstrate line-narrowed EO PPLN Q-switched laser with intra-cavity optical parametric oscillation using a grazing-incidence grating. The grazing-incidence grating acts as an important role to significantly reduce the spectral width of the output signal. The energy per unit spectral width is increased from 10.1 μJ/4 nm to 5 μJ/0.03 nm when pumped with 10-W pump power. Wavelength tuning is achieved by rotating the rear reflector and changing the crystal temperature.

The authors thank Yen-Chieh Huang and Shou-Tai Lin for their useful suggestions and discussions. This work was supported by National Science Council, Taiwan under contract NSC102-2221-E-007-100-MY2.

References

1. L. E. Myers and W. R. Bosenberg, IEEE J. Quantum Electron. **33,** 1663 (1997).
2. X. P. Hu, P. Xu, and S. N. Zhu, Photon. Res. **1,** 171 (2013).
3. Y. Tang, Y. Chen, H. Jiang, W. Ji, Y. Wu, and X. Chen, Chin. Opt. Lett. **11,** 061901 (2013).
4. L. Ye, J. Wang, H. Hu, J. Yu, and K. Song, Chin. Opt. Lett. **11,** 110604 (2013).
5. Y. H. Chen and Y. C. Huang, Opt. Lett. **28,** 1460 (2003).
6. Y. Y. Lin, S. T. Lin, G. W. Chang, A. C. Chiang, and Y. C. Huang, Opt. Lett. **31,** 545 (2007).
7. Y. H. Chen, Y. C. Huang, Y. Y. Lin, and Y. F. Chen, Appl. Phys. B **80,** 889 (2005).

8. S. T. Lin, G. W. Chang, Y. Y. Lin, Y. C. Huang, A. C. Chiang, and Y. H. Chen, Opt. Express **15,** 17093 (2007).
9. A. C. Chiang and Y. Y. Lin, Chin. Phys. Lett. **30,** 094201 (2013).
10. A. C. Chiang, T. D. Wang, Y. Y. Lin, C. W. Liu, Y. H. Chen, B. C. Wong, Y. C. Huang, IEEE J. Quantum Electron. **40,** 791 (2004).
11. D J. M. Stothard, C. F. Rae, and M. H. Dunn, IEEE J. Quantum Electron. **45,** 256 (2009).
12. C. S. Yu and A. H. Kung, J. Opt. Soc. Am. B **16,** 2233 (1999).
13. W. R. Bosenberg, A. Drobshoff, J. I. Alexander, L. E. Myers, and R. L. Byer, Opt. Lett. **21,** 1336 (1996).
14. T. Debuisschert, J. Raffy, J. P. Pocholle, and M. Papuchon, J. Opt. Soc. Am. B **13,** 1569 (1996).
15. D. E. Zelmon, D. L. Small, and D. Jundt, J. Opt. Soc. Amer. B, Opt. Phys. **14,** 3319 (1997).